

# Bark-dwelling methanotrophic bacteria decrease methane emissions from trees

Luke C Jeffrey (✉ [luke.jeffrey@scu.edu.au](mailto:luke.jeffrey@scu.edu.au))

Southern Cross University <https://orcid.org/0000-0001-6536-6757>

Damien T. Maher

Southern Cross University <https://orcid.org/0000-0003-1899-005X>

Eleonora Chiri

Monash University <https://orcid.org/0000-0002-6627-0762>

Pok Man Leung

Monash University <https://orcid.org/0000-0002-5382-827X>

Philipp A. Nauer

Monash University <https://orcid.org/0000-0003-2237-9106>

Stefan K. Arndt

University of Melbourne <https://orcid.org/0000-0001-7086-9375>

Douglas R. Tait

Southern Cross University <https://orcid.org/0000-0001-7690-7651>

Chris Greening

Monash University <https://orcid.org/0000-0001-7616-0594>

Scott G. Johnston

Southern Cross University <https://orcid.org/0000-0002-5826-5613>

---

## Research Article

**Keywords:** Tree stem methane, MOB, methanotroph, carbon cycle, lowland forests, wetlands, greenhouse gases, microbe, methanogen, isotope, Methylomonas, methane emissions

**Posted Date:** December 3rd, 2020

**DOI:** <https://doi.org/10.21203/rs.3.rs-119818/v1>

**License:**  This work is licensed under a Creative Commons Attribution 4.0 International License.

[Read Full License](#)

---

# Abstract

Tree stems are an important and unconstrained source of methane, yet it is uncertain if there are internal microbial controls (i.e. methanotrophy) within tree bark, that may reduce methane emissions. Using multiple lines of evidence, we demonstrate here that unique microbial communities dominated by methane oxidising bacteria (MOB) dwell within bark of *Melaleuca quinquenervia*, a common, invasive and globally distributed lowland species. Laboratory incubations of methane inoculated *M. quinquenervia* bark reveal methane consumption (up to  $96.3 \mu\text{mol m}^{-2} \text{ bark d}^{-1}$ ) and distinct isotopic  $\delta^{13}\text{C-CH}_4$  enrichment characteristic of MOB. Molecular analysis indicates unique microbial communities reside within the bark, with methane-oxidising bacteria primarily from the genus *Methylomonas* comprising up to 25 % of the total microbial community. Methanotroph abundance was linearly correlated to methane uptake rates ( $R^2 = 0.76$ ,  $p = 0.006$ ). Finally, field-based methane oxidation inhibition experiments demonstrate that bark-dwelling MOB reduce methane emissions by  $36 \pm 5$  %. These multiple, complementary lines of evidence indicate that bark-dwelling MOB represent a novel and potentially significant methane sink, and an important frontier for further research.

## Key Points

- The bark of a common wetland tree species contains a unique microbial community containing up to 25 % methane-oxidising bacteria (MOB)
- Bark-dwelling MOB can decrease tree methane emissions by  $\sim 36$  %
- MOB abundance in bark strongly predicted methane oxidation rates
- Tree bark MOB represent a novel, substantial and previously unrecognised methane sink

## Main Text

Methane ( $\text{CH}_4$ ) is  $\sim 32$  to  $87$  times more potent than carbon dioxide at warming the Earth's atmosphere<sup>6</sup>. Methane emissions from tree stems has received growing attention and is considered a new frontier in the global carbon cycle<sup>1</sup>. With an estimated three trillion trees on Earth<sup>7</sup> and reforestation / afforestation promoted as viable climate change mitigation strategies<sup>8-11</sup>, a mechanistic understanding of the processes driving and moderating methane emission from trees is of critical importance. Freshwater wetland trees typically emit much higher rates of methane<sup>4, 12</sup> than their mangrove<sup>13</sup> and upland forest counterparts<sup>14-18</sup>. This is because the poorly drained, carbon-rich soils typical of freshwater wetland forests are favourable for methanogenesis. Recent research revealed that lowland trees contributed  $\sim 50$  % of the Amazon methane emission budget<sup>4</sup>, highlighting the potential importance of this emission pathway. However, a lack of data on tree-mediated methane emissions has prevented their inclusion in global methane budgets<sup>3</sup>.

Methane-oxidizing bacteria (MOB) can decrease methane emissions in a wide range of natural environments. Wetlands are recognised as Earth's largest natural source of atmospheric methane<sup>3, 19</sup>, however 50-90 % of the methane produced within wetlands may be oxidised before reaching the atmosphere<sup>20-22</sup>. Although the importance of MOB within wetland soil and water is well documented<sup>22-27</sup>, their possible role within trees has yet to be characterised. Methanogenic bacteria have been identified within the heartwood and sapwood of several lowland tree species<sup>28-31</sup>, but the operational taxonomic units of methanotrophic families were exceedingly rare<sup>29</sup> and their influence on tree stem methane emissions remains unquantified. Until now, it is unclear if bark may provide a novel habitat for MOB.

Here, we establish that tree stem bark can host a previously uncharacterised, novel microbiome and unique MOB community, which may substantially mitigate tree stem methane emissions and thereby help regulate Earth's climate. Our study combined the use carbon stable isotope analysis<sup>23, 27, 32, 33</sup>, *in situ* methanotrophy inhibitors<sup>34, 35</sup>, and molecular community profiling<sup>36, 37</sup>, which have each been previously used to determine the rates and mediators of microbial oxidation in wetlands and other environments. On this basis, we provide multiple lines of biogeochemical and microbial evidence that abundant MOB occupy tree bark and represent a novel methane sink.

### **Methane oxidation and fractionation during bark incubations**

In order to detect MOB activity, we monitored methane concentrations and isotope fractionation in methane-inoculated gas-tight bottles containing freshly collected *M. quinquenervia* bark samples, from three different sites (see Supplementary Methods). Because the heavier <sup>13</sup>C-CH<sub>4</sub> isotope contains slightly stronger bonds, MOB preferentially consume <sup>12</sup>C-CH<sub>4</sub>, thereby triggering isotopic fractionation. Two laboratory time series experiments both revealed clear methane consumption coupled to δ<sup>13</sup>C-CH<sub>4</sub> enrichment (Fig. 1). There was considerable variation in methane oxidation rates between sampled trees of the second experiment, with methane uptake ranging from 4.8 to 81.2 μmol m<sup>-2</sup> bark d<sup>-1</sup> (Table S1). No methane consumption or fractionation occurred within blank controls and sterilised (microwaved) bark treatments (Fig. 1). The average fractionation factor (α) observed between the bark samples was similar across the three sampled sites (MF1: 1.040 ± 0.013; FF1: 1.031 ± 0.005; FF2: 1.033 ± 0.017; Fig. 1, Table S1). The fractionation factors were generally higher than reported literature values for MOB including those reported for upland temperate forested soils (α=1.018-1.022)<sup>38, 39</sup> and tropical forested soils (1.012-1.023)<sup>40</sup>, but were within range of both subtropical wetlands (α=1.003-1.032)<sup>23, 41</sup> and rice paddies (α=1.013-1.033)<sup>42, 43</sup> (Table S2). Our lab-based fractionation factor α values may be higher due to methane inoculation concentrations differing to natural field conditions<sup>44</sup> or may reflect the relatively high community abundance of bark-dwelling MOB found in paired samples (see microbial data in Fig. 2).

## Methane oxidation is strongly correlated with MOB abundance in tree bark

Molecular analysis was used to determine the abundance (quantitative PCR) and composition (amplicon sequencing) of the total bacterial communities (*via* universal 16S rRNA gene) and MOB communities (*via* *pmoA* gene encoding a particulate methane monooxygenase subunit) within tree bark samples (n = 14). The marker gene for aerobic methanotrophy (*pmoA*) was detected in relatively high abundance in every sample (av.  $2 \times 10^9$  copies per gram of dry sample material; range of  $4 \times 10^7$  to  $5 \times 10^9$ ; Fig. 2a), with values comparable to wetland sediments<sup>45</sup>. The relative abundance of MOB was remarkably high within the bark microbial communities (5.4 to 24.7 % based on qPCR, Fig. 2c; 3.2 to 12.8 % based on amplicon sequencing, Fig. 2d). This is in stark contrast to the reported low MOB abundance in the heartwood and sapwood of other tree species (<0.1 %, *Populus deltoids*)<sup>29</sup>. Compositional profiling revealed that the bark samples hosted unique microbial communities that were distinct from those in adjacent sediments and waters (Fig. 2b; Fig. S2;  $p < 0.001$ ) and likely adapted to the acidic pH observed in the bark<sup>46</sup>. Over half of the total bacterial community comprised five genera, *Mycobacterium*, *Acidocella*, *Occallatibacter*, *Conexibacter* and the MOB genus *Methylomonas* (Fig. 2f; Fig. S2). Consistently, *Methylomonas* accounted for the majority of the methanotrophic community based on analysis of the total bacterial community (Fig. 2e) and MOB community (Fig. S3). Other acidophilic members of the genus are known to be associated with *Sphagnum* mosses and have been shown to significantly mitigate methane emissions from wetlands<sup>37, 46</sup>, suggesting *Methylomonas* are well-adapted to vegetation-associated lifestyles. Several trees also hosted a large proportion of a novel lineage of Methylacidiphilaceae, a family of acidophilic methanotrophs from the phylum Verrucomicrobia<sup>47-49</sup> (Fig. 2e), thus expanding the tree MOB niche to at least two phyla. Remarkably, MOB abundance determined by qPCR and 16S rRNA amplicon sequencing strongly predicted methane oxidation rates with paired bark samples (T1-T7) from FF2 ( $R^2 = 0.76$  and  $0.74$  respectively; Figs. 2c & 2d). Thus, tree-bark methane oxidation rates are well-explained by the high yet variable abundance of bark-associated *Methylomonas*.

## Field-based MOB inhibition confirms novel methane sink activity within bark

To both confirm and quantify the MOB activity moderating tree stem methane emissions *in situ*, we utilised DFM inhibition experiments on *M. quinquenervia* tree stems (n = 88). The use of specific inhibitors of methanotrophy enable estimation of methane oxidation rates by MOB under both lab- and field-based conditions<sup>34, 35, 50, 51</sup>. Low concentrations of difluoromethane ( $\text{CH}_2\text{F}_2$ ; DFM) temporarily and effectively inhibit methanotrophy by competing with methane as a substrate for methane monooxygenase<sup>35, 52</sup> (the major enzyme catalysing aerobic methane oxidation), without affecting methanogenesis<sup>34</sup>. To achieve this, replicate baseline tree stem methane fluxes were measured before (Fig. S1a) and then ~1 hour after the addition of DFM (Fig. S1b) into tree flux chambers<sup>33</sup> (see Supplementary Methods for more information). A net positive change in methane fluxes was observed in nearly all chambers after the addition of DFM (average increase of  $36.3 \pm 5.4$  %), indicating MOB were

present, active, and effectively inhibited (Fig. 3). The changes in blank (control) repeated chamber measurements ( $n = 39$ ) - without the addition of DFM over a similar incubation period - were normally distributed around zero (mean of  $3.1 \pm 2.5$  %) and significantly different to the MOB inhibited DFM measurements ( $p < 0.001$ , Fig. 3). These results provide a first order estimate of *in situ* bark dwelling MOB activity mitigating  $\sim 36$  % of the methane emissions from tree stems.

## Conclusion

This study provides the first conclusive evidence of active methane oxidation by a unique MOB community, within the bark of a widely distributed wetland tree species. This important discovery adds to our evolving understanding of tree mediated methane fluxes. If MOB are a ubiquitous feature within methane emitting trees, our conceptual understanding of the global methane cycle may need revision. Constraining the relative importance, distribution and magnitude of MOB in mediating methane emissions from trees, should therefore be a focus of future work in this frontier research area.

## References

1. Barba J, Bradford MA, Brewer PE, Bruhn D, Covey K, van Haren J, et al. Methane emissions from tree stems: a new frontier in the global carbon cycle. *New Phytologist*. 2019;222(1):18-28.
2. Covey KR, Megonigal JP. Methane production and emissions in trees and forests. *New Phytologist*. 2019;222(1):35-51.
3. Saunois M, Stavert AR, Poulter B, Bousquet P, Canadell JG, Jackson RB, et al. The Global Methane Budget 2000-2017. *Earth System Science Data Discussions*. 2019:1-138.
4. Pangala SR, Enrich-Prast A, Basso LS, Peixoto RB, Bastviken D, Hornibrook ER, et al. Large emissions from floodplain trees close the Amazon methane budget. *Nature*. 2017;552(7684):230.
5. Machacova K, Borak L, Agyei T, Schindler T, Soosaar K, Mander Ü, et al. Trees as net sinks for methane ( $\text{CH}_4$ ) and nitrous oxide ( $\text{N}_2\text{O}$ ) in the lowland tropical rain forest on volcanic Réunion Island. *New Phytologist*.
6. Neubauer SC, Megonigal JP. Moving beyond global warming potentials to quantify the climatic role of ecosystems. *Ecosystems*. 2015;18(6):1000-13.
7. Crowther TW, Glick HB, Covey KR, Bettigole C, Maynard DS, Thomas SM, et al. Mapping tree density at a global scale. *Nature*. 2015;525(7568):201.
8. Arora VK, Montenegro A. Small temperature benefits provided by realistic afforestation efforts. *Nature Geoscience*. 2011;4(8):514-8.
9. Lewis SL, Wheeler CE, Mitchard ET, Koch A. Restoring natural forests is the best way to remove atmospheric carbon. *Nature Publishing Group*; 2019.
10. Griscom BW, Adams J, Ellis PW, Houghton RA, Lomax G, Miteva DA, et al. Natural climate solutions. *Proceedings of the National Academy of Sciences*. 2017;114(44):11645-50.

11. House JI, Colin Prentice I, Le Quere C. Maximum impacts of future reforestation or deforestation on atmospheric CO<sub>2</sub>. *Global Change Biology*. 2002;8(11):1047-52.
12. Sjögersten S, Siegenthaler A, Lopez OR, Aplin P, Turner B, Gauci V. Methane emissions from tree stems in neotropical peatlands. *New Phytologist*. 2019.
13. Jeffrey LC, Reithmaier G, Sippo JZ, Johnston SG, Tait DR, Harada Y, et al. Are methane emissions from mangrove stems a cryptic carbon loss pathway? Insights from a catastrophic forest mortality. *New Phytologist*. 2019.
14. Covey KR, Wood SA, Warren RJ, Lee X, Bradford MA. Elevated methane concentrations in trees of an upland forest. *Geophysical Research Letters*. 2012;39(15).
15. Megonigal JP, Guenther AB. Methane emissions from upland forest soils and vegetation. *Tree physiology*. 2008;28(4):491-8.
16. Wang ZP, Gu Q, Deng FD, Huang JH, Megonigal JP, Yu Q, et al. Methane emissions from the trunks of living trees on upland soils. *New Phytol*. 2016;211(2):429-39.
17. Welch B, Gauci V, Sayer EJ. Tree stem bases are sources of CH<sub>4</sub> and N<sub>2</sub>O in a tropical forest on upland soil during the dry to wet season transition. *Global Change Biology*. 2018;25(1):361-72.
18. Machacova K, Back J, Vanhatalo A, Halmeenmaki E, Kolari P, Mammarella I, et al. *Pinus sylvestris* as a missing source of nitrous oxide and methane in boreal forest. *Scientific Reports*. 2016;6:23410.
19. Bartlett KB, Harriss RC. Review and assessment of methane emissions from wetlands. *Chemosphere*. 1993;26(1-4):261-320.
20. Oremland RS, Culbertson CW. Importance of methane-oxidizing bacteria in the methane budget as revealed by the use of a specific inhibitor. *Nature*. 1992;356(6368):421-3.
21. King GM. Regulation by light of methane emissions from a wetland. *Nature*. 1990;345(6275):513-5.
22. Segarra K, Schubotz F, Samarkin V, Yoshinaga M, Hinrichs K, Joye S. High rates of anaerobic methane oxidation in freshwater wetlands reduce potential atmospheric methane emissions. *Nature communications*. 2015;6:7477.
23. Jeffrey LC, Maher DT, Johnston SG, Kelaher BP, Steven A, Tait DR. Wetland methane emissions dominated by plant-mediated fluxes: Contrasting emissions pathways and seasons within a shallow freshwater subtropical wetland. *Limnology and Oceanography*. 2019.
24. Tyler SC, Bilek RS, Sass RL, Fisher FM. Methane oxidation and pathways of production in a Texas paddy field deduced from measurements of flux,  $\delta^{13}\text{C}$ , and  $\delta\text{D}$  of CH<sub>4</sub>. *Global Biogeochemical Cycles*. 1997;11(3):323-48.
25. Valentine DL. Biogeochemistry and microbial ecology of methane oxidation in anoxic environments: a review. *Antonie Van Leeuwenhoek*. 2002;81(1-4):271-82.
26. Valenzuela EI, Prieto-Davó A, López-Lozano NE, Hernández-Eligio A, Vega-Alvarado L, Juárez K, et al. Anaerobic methane oxidation driven by microbial reduction of natural organic matter in a tropical wetland. *Applied and Environmental Microbiology*. 2017;83(11):e00645-17.

27. Chanton JP. The effect of gas transport on the isotope signature of methane in wetlands. *Organic Geochemistry*. 2005;36(5):753-68.
28. Zeikus J, Henning DL. *Methanobacterium arbophilicum* sp. nov. An obligate anaerobe isolated from wetwood of living trees. *Antonie van Leeuwenhoek*. 1975;41(1):543-52.
29. Yip DZ, Veach AM, Yang ZK, Cregger MA, Schadt CW. Methanogenic Archaea dominate mature heartwood habitats of Eastern Cottonwood (*Populus deltoides*). *New Phytologist*. 2018.
30. Schink B, Ward JC, Zeikus JG. Microbiology of wetwood: importance of pectin degradation and *Clostridium* species in living trees. *Applied and environmental microbiology*. 1981;42(3):526-32.
31. Flanagan LB, Nikkel DJ, Scherloski LM, Tkach RE, Smits KM, Selinger LB, et al. Multiple processes contribute to methane emission in a riparian cottonwood forest ecosystem. *New Phytologist*.
32. Maher DT, Cowley K, Santos IR, Macklin P, Eyre BD. Methane and carbon dioxide dynamics in a subtropical estuary over a diel cycle: Insights from automated in situ radioactive and stable isotope measurements. *Marine Chemistry*. 2015;168:69-79.
33. Jeffrey LC, Maher DT, Tait DR, Johnston SG. A Small Nimble In Situ Fine-Scale Flux Method for Measuring Tree Stem Greenhouse Gas Emissions and Processes (S.N.I.F.F.). *Ecosystems*. 2020.
34. Vicca S, Flessa H, Loftfield N, Janssens I. The inhibitory effect of difluoromethane on CH<sub>4</sub> oxidation in reconstructed peat columns and side-effects on CO<sub>2</sub> and N<sub>2</sub>O emissions at two water levels. *Soil Biology and Biochemistry*. 2009;41(6):1117-23.
35. Miller LG, Sasson C, Oremland RS. Difluoromethane, a new and improved inhibitor of methanotrophy. *Applied and Environmental Microbiology*. 1998;64(11):4357-62.
36. Chiri E, Greening C, Lappan R, Waite DW, Jirapanjawat T, Dong X, et al. Termite mounds contain soil-derived methanotroph communities kinetically adapted to elevated methane concentrations. *The ISME Journal*. 2020;14(11):2715-31.
37. Kip N, Dutilh BE, Pan Y, Bodrossy L, Neveling K, Kwint MP, et al. Ultra-deep pyrosequencing of pmoA amplicons confirms the prevalence of *Methylobacter* and *Methylocystis* in Sphagnum mosses from a Dutch peat bog. *Environmental microbiology reports*. 2011;3(6):667-73.
38. Tyler SC, Crill PM, Brailsford GW. <sup>13</sup>C/<sup>12</sup>C Fractionation of methane during oxidation in a temperate forested soil. *Geochimica et Cosmochimica Acta*. 1994;58(6):1625-33.
39. Snover AK, Quay PD. Hydrogen and carbon kinetic isotope effects during soil uptake of atmospheric methane. *Global Biogeochemical Cycles*. 2000;14(1):25-39.
40. Teh YA, Silver WL, Conrad ME. Oxygen effects on methane production and oxidation in humid tropical forest soils. *Global Change Biology*. 2005;11(8):1283-97.
41. Happell JD, Chanton JP, Showers WS. The influence of methane oxidation on the stable isotopic composition of methane emitted from Florida swamp forests. *Geochimica et Cosmochimica Acta*. 1994;58(20):4377-88.
42. Zhang G, Yu H, Fan X, Ma J, Xu H. Carbon isotope fractionation reveals distinct process of CH<sub>4</sub> emission from different compartments of paddy ecosystem. *Scientific reports*. 2016;6(1):1-10.

43. Zhang G, Ji Y, Ma J, Liu G, Xu H, Yagi K. Pathway of CH<sub>4</sub> production, fraction of CH<sub>4</sub> oxidized, and <sup>13</sup>C isotope fractionation in a straw-incorporated rice field. *Biogeosciences*. 2013;10(5):3375.
44. Templeton AS, Chu K-H, Alvarez-Cohen L, Conrad ME. Variable carbon isotope fractionation expressed by aerobic CH<sub>4</sub>-oxidizing bacteria. *Geochimica et Cosmochimica Acta*. 2006;70(7):1739-52.
45. Yun J, Yu Z, Li K, Zhang H. Diversity, abundance and vertical distribution of methane-oxidizing bacteria (methanotrophs) in the sediments of the Xianghai wetland, Songnen Plain, northeast China. *Journal of Soils and Sediments*. 2013;13(1):242-52.
46. Kip N, Ouyang W, van Winden J, Raghoebarsing A, van Niftrik L, Pol A, et al. Detection, isolation, and characterization of acidophilic methanotrophs from Sphagnum mosses. *Applied and Environmental Microbiology*. 2011;77(16):5643-54.
47. Carere CR, Hards K, Houghton KM, Power JF, McDonald B, Collet C, et al. Mixotrophy drives niche expansion of verrucomicrobial methanotrophs. *The ISME journal*. 2017;11(11):2599-610.
48. Pol A, Heijmans K, Harhangi HR, Tedesco D, Jetten MS, Den Camp HJO. Methanotrophy below pH 1 by a new Verrucomicrobia species. *Nature*. 2007;450(7171):874-8.
49. van Teeseling MC, Pol A, Harhangi HR, van der Zwart S, Jetten MS, den Camp HJO, et al. Expanding the verrucomicrobial methanotrophic world: description of three novel species of *Methylacidimicrobium* gen. nov. *Applied and environmental microbiology*. 2014;80(21):6782-91.
50. Chan A, Parkin T. Evaluation of potential inhibitors of methanogenesis and methane oxidation in a landfill cover soil. *Soil Biology and Biochemistry*. 2000;32(11-12):1581-90.
51. Urmann K, Schroth MH, Zeyer J. Recovery of in-situ methanotrophic activity following acetylene inhibition. *Biogeochemistry*. 2008;89(3):347-55.
52. Nauer PA, Hutley LB, Arndt SK. Termite mounds mitigate half of termite methane emissions. *Proceedings of the National Academy of Sciences*. 2018;115(52):13306-11.

## Methods

### ***In situ* tree stem methane flux rates and bark preparation**

*Melaleuca quinquenervia* stem fluxes were determined using a small chamber directly attached to the tree with a portable cavity ring-down spectrometer (G4302-GasScouter, Picarro)<sup>33</sup> from forests in subtropical, north-eastern NSW, Australia. During the first stable isotope MOB experiment, paired tree stem bark samples were collected from opposite sides of four *M. quinquenervia* trees with high methane fluxes, spanning two sites with differing hydrological characteristics. One site featured moist sediments (MF1) around the tree base (n = 4) whereas the other was completely inundated with freshwater ~50 cm up the tree stem (n = 5) (FF1). Within one hour of bark sample collection, each sample was weighed (with samples ranging from 81 to 147 g; Table S1) and then volumetrically measured with a ruler (cm<sup>3</sup>). The bark samples were then cut into sufficiently narrow strips (~1 cm) to fit through the bottle-neck of sterile (autoclaved) 550 mL crimp top glass bottles. Care was taken to ensure minimal disturbance to the planar

bark layers to preserve as much of the natural bark microstructure as possible. Each bottle was then capped, wrapped in aluminium foil and inoculated with 101 ppm CH<sub>4</sub> in air gas standard (CoreGas). This was achieved by flushing each bottle for six minutes using a two-syringe system, featuring a long inlet syringe reaching near the bottom of the bottle and a short venting syringe evacuating the headspace closer to the top of each bottle. Four bark-free empty bottles (blanks) were used as controls, and were also wrapped, crimped and flushed using the same 101 ppm CH<sub>4</sub> standard and methods.

A repeat experiment (FF2), focused solely on an inundated forest site, utilised seven trees spanning a range in CH<sub>4</sub> flux rates (1.1 to 393 mmol m<sup>-2</sup> d<sup>-1</sup>) (Table S1). Larger bark samples (approximately 13 x 25 cm) from the lower stem of trees in standing water that was on average 54.0 ± 12.9 cm deep, were extracted using sterile methods and then cut into thirds. For the microbial analysis, one third of each bark sample was field-wrapped in sterile foil pockets (pre-baked at 180°C for 6 hours) immediately after extraction, and then placed on ice (n = 7). Ancillary composite sediment and surface water samples were also collected using sterile methods. All samples were refrigerated within two hours of collection at 4 °C. They were later transported with dry ice to Monash University (Greening Lab) for the microbial analysis. One third of each bark sample was prepared as per first experiment methods (n = 7) and were placed into sealed crimp top sterile bottles. The final third of bark sample from each tree were placed in sterile crimp top bottles, but microbial communities were neutralised by microwaving (1600W – LG model MS3882XRSK) for 2 minutes, four times over, before sealing (n = 7). All paired samples (i.e. raw bark and microwaved control) were then inoculated with 101 ppm methane as per the syringe method above.

### **Isotope time series inoculation experiment**

The headspace concentration of CH<sub>4</sub> and δ<sup>13</sup>C-CH<sub>4</sub> of the inoculated bark bottles, the neutralised bark bottles and blanks were sampled using a cavity ring-down spectrometer (CRDS) with a sensitivity of 5 ppb + 0.05 % of reading (<sup>12</sup>C), 1 ppb + 0.05 % of reading (<sup>13</sup>C) (Picarro, G2201-i). At 3 to 24 hourly intervals (increasing with experiment duration), a 60 mL gas sample of 101 ppm CH<sub>4</sub> was injected into the bottle septum using a long syringe needle, whilst simultaneously mixing and removing 60 mL of gas sample via a second and short syringe needle. To ensure adequate headspace mixing occurred, headspace mixing was repeated at least eight times before extracting each sample (i.e. the volume of gas mixed was greater than the headspace volume within each bottle). The extracted gas sample was then analysed directly from the syringe into the CRDS. The sample concentration of CH<sub>4</sub> (ppm), δ<sup>13</sup>C-CH<sub>4</sub> (‰) and the associated ±SD were recorded for each bottle treatment at each time interval. The 60 mL mixing additions of CH<sub>4</sub> and δ<sup>13</sup>C-CH<sub>4</sub> (‰) to each bottle headspace were later accounted for via mass balance, to calculate the shift in CH<sub>4</sub> and δ<sup>13</sup>C-CH<sub>4</sub> (‰) over time. The decrease in CH<sub>4</sub> over the first 24 hours was converted to uptake, as a proportion of the original surface area of each bark treatment within each bottle. The fractionation factor (α) was defined as the ratio of the oxidation rate coefficients of <sup>12</sup>CH<sub>4</sub> over <sup>13</sup>CH<sub>4</sub>, and calculated using established methods<sup>53</sup>.

### **Genomic DNA extraction**

High-quality and amplifiable genomic DNA were extracted from all bark (n = 14), sediment (n = 3) and water (n = 6) samples. For each individual bark sample, 0.13 to 0.18 g (wet weight) of material was frozen in liquid nitrogen and immediately homogenised using a sterile pestle and mortar until a fine powder was obtained. Genomic DNA was extracted from the homogenised samples using the Synergy 2.0 Plant DNA Extraction Kit (OPS Diagnostics LLC, US), according to the manufacturer's instructions. Genomic DNA from the sediment samples (0.25 g wet weight sample) and water samples (50 mL sample filtered on to sterile filter papers) were extracted using the DNeasy PowerSoil Kit (Qiagen, US), according to the manufacturer's instructions. The purity and yield of the DNA extracts were verified by spectrophotometry (NanoDrop ND-1000 spectrophotometer, Nanodrop Technologies Inc., US) and quantified by fluorometry (Qubit Fluorometer, Thermo Fisher Scientific). For the DNA extraction from each type of sample, PCR-grade water was extracted as a negative control.

### Quantitative PCR

Quantitative PCR assays were performed on a QuantStudio 7 Flex Real-Time PCR instrument (Thermo Fisher Scientific), to quantify gene copy numbers and estimate the abundance of the total microbial (16S rRNA gene copies) and MOB community (*pmoA* gene copies). Briefly, the *pmoA* gene was amplified using the previously described degenerate primers A189f 5'-GGNGACTGGGACTTCTGG-3' and mb661 5'-CCGGMGCAACGTCYTTACC-3'<sup>54, 55</sup> and cycling conditions<sup>56</sup>. The primers pair was chosen for its coverage of the MOB community from environments with elevated CH<sub>4</sub> concentrations. The V4 hypervariable region of the 16S rRNA gene was amplified using the universal Earth Microbiome Project primer pairs 515FB 5'-GTGYCAGCMGCCGCGTAA-3' and 806RB 5'-GGACTACNVGGGTWTCTAAT-3'<sup>57</sup>, as per previously described cycling conditions<sup>58</sup>. The employed reaction conditions and thermal profiles of the qPCR assays have been previously described<sup>36</sup>. Amplification from different dilutions (from undiluted to 1:100 dilution in PCR-grade water) of DNA extracts was tested, and the dilution resulting in the highest yield and quality of PCR product was used for the qPCR assays. For each assay (96-well plate), duplicate serial dilutions of quantified 16S rRNA gene (from *Escherichia coli*) or *pmoA* gene amplicons, (from *Methylosinus trichosporium* strain OB3b) were used to generate standard calibration curves. Each sample was analysed in triplicate; amplification efficiencies (>70 %) were calculated from the slopes of the calibration curves (R<sup>2</sup> values > 0.97). No significant amplification of the blank extractions was observed in any qPCR assays.

### Amplicon sequencing

Amplicon sequencing of the universal 16S rRNA gene was used to infer the community composition of the total bacterial and archaeal community within each sample. Amplicon sequencing of the *pmoA* gene, encoding the particulate methane monooxygenase A subunit, was also performed to gain a higher-resolution insight into the composition of the MOB community. Genomic DNA extracts of 14 bark, two composite sediment and two composite water samples (pooled samples), as well as the blank extraction, were subject to Illumina MiSeq paired-end sequencing at the Australian Centre for Ecogenomics, University of Queensland. The resultant raw sequences from the 16S rRNA gene amplicon sequencing

were subject to quality filtering, merging, primer trimming, denoising and singleton removal using the QIIME 2 platform<sup>59</sup>. Taxonomic affiliation of the identified amplicon sequence variants (16S-ASVs) was assigned according to the GTDB taxonomy<sup>60</sup>. For each sample, 16S-ASVs classified as “unassigned” (av. 5.2 %), “Eukaryota” (av. 0.04 %), “Chloroplast” (av. 1.7 %), and “Mitochondria” (av. 0.3 %) were excluded as potentially derived from plant material. The final dataset accounted for 2727 16S-ASVs, with an average sequence count number per sample of 9184 (range 3657 in sample T6.2 to 14524 in sample S2). The 16S-ASVs assigned to known methanotrophic families and genera were subset to infer MOB community structure and to estimate the proportion of the MOB community within the total microbial community via the 16S-ASV dataset. Note that this analysis cannot detect uncultured MOB with unknown 16S rRNA gene sequences. Data processing of the *pmoA* gene amplicon sequences followed our previously published pipeline<sup>36, 61</sup>, with minor modifications. All processing steps were performed in the QIIME 2 platform and, instead of assigning the raw sequences to operational taxonomic units, raw sequences were denoised using the DADA2 pipeline<sup>62</sup>, yielding 280 high-quality *pmoA* amplicon sequence variants (*pmoA*-ASVs). Taxonomic affiliation of the *pmoA*-ASVs was assigned by similarity with *pmoA* sequences of a curated database<sup>63</sup>. The average sequence count number per sample was 8556; range 5026 in sample T7.1 to 14729 in sample T5.1. Sample T6.2, with a sequence count number of 1503, was excluded from further analyses. Note that this analysis cannot detect highly divergent MOB *pmoA* sequences, such as those from Verrucomicrobiota and *Candidatus* Methyloimabilota.

## Microbial diversity analyses

To assess total and MOB community structure based on both 16S-ASV and *pmoA*-ASV dataset, read count normalisation and alpha and beta diversity calculations were performed with the package phyloseq v1.30<sup>64</sup> from the open source software Bioconductor. Chao1, Shannon and Inverse Simpson indices were computed to assess the alpha diversity of total and MOB communities, whereas beta diversity was measured using the Bray–Curtis distance matrix<sup>65</sup> and visualised using non-parametric multidimensional scaling ordinations (nMDS). To determine whether the observed between-group distances were statistically significant, we performed permutational multivariate analysis of variance (PERMANOVA) with the software PRIMER-E v7 (PRIMER-E Ltd., Plymouth, United Kingdom). For bark samples, correlations between *pmoA* and 16S rRNA gene abundance, qPCR- and 16S-ASV-based MOB community proportion, and CH<sub>4</sub> uptake and *in situ* tree stem CH<sub>4</sub> fluxes were tested for significance using linear regression, after appropriate variable transformations (log<sub>10</sub> for gene abundances, logit for MOB community proportion) and removal of outliers as indicated by diagnostic plots (qq- and Cook’s distance). Correlations between qPCR- and 16S-ASV-based MOB community proportion and CH<sub>4</sub> uptake were highly significant ( $p < 0.008$ ).

## *In situ* methanotroph inhibitor experiments with difluoromethane (DFM)

The *in situ* MOB oxidation rates were estimated by first measuring duplicate un-inoculated tree stem fluxes using the ‘Small Nimble *In situ* Fine-scale Flux’ (S.N.I.F.F.) method<sup>33</sup> (n = 88 trees). Then the tree

stem chamber was flushed with atmospheric air for 30 seconds or until atmospheric concentration in the chamber was attained, and 120 mL addition of 2 % difluoromethane (DFM) was slowly injected, then sealed within each chamber and left to incubate and infiltrate the bark for ~45 – 90 minutes, similar to a sufficient time previously shown to inhibit MOB<sup>34</sup>. The chamber was then again flushed again with atmospheric air and then duplicate methane flux rates were measured. As DFM has been shown to be an effective inhibitor of aerobic methanotrophy<sup>35</sup>, the difference between initial methane fluxes and the subsequent DFM inoculated fluxes were deemed to be the effect of inhibition of MOB<sup>52</sup>. Blank repeated chamber flux measurements with no DFM injections were also performed *in situ* to ensure no enhancement of methane fluxes occurred, as a result of repeated chamber measurement at the same location (n = 39). Closed loop experiments conducted in the laboratory spanning a spectrum of methane concentrations (1.8 – 400 ppm) revealed no increase in methane concentrations occurred when adding 2 % DFM when using a CRDS (Picarro, GasScouter G4301). Occasionally, interference with the H<sub>2</sub>O sensor was observed, but never under field conditions when DFM was left to incubate and diffuse. Shapiro-Wilk normality tests were used to determine whether the % change in DFM and blank repeat CH<sub>4</sub> flux treatments were non-parametric ( $p < 0.05$ ) and had equal variance ( $p < 0.05$ ), using Sigmaplot 13.0. A Kruskal-Wallis One Way Analysis of Variance on Ranks was then used to determine whether there was a significant difference between the treatments and Dunn's Method was then used isolate the group/s that differed from the others, using pairwise multiple comparison procedures, where statistically significant differences were  $p < 0.001$ .

## Methods References

53. Coleman DD, Risatti JB, Schoell M. Fractionation of carbon and hydrogen isotopes by methane-oxidizing bacteria. *Geochimica et Cosmochimica Acta*. 1981;45(7):1033-7.
54. Holmes AJ, Costello A, Lidstrom ME, Murrell JC. Evidence that participate methane monooxygenase and ammonia monooxygenase may be evolutionarily related. *FEMS microbiology letters*. 1995;132(3):203-8.
55. Costello AM, Lidstrom ME. Molecular characterization of functional and phylogenetic genes from natural populations of methanotrophs in lake sediments. *Applied and environmental microbiology*. 1999;65(11):5066-74.
56. Henneberger R, Chiri E, Bodelier PE, Frenzel P, Lüke C, Schroth MH. Field-scale tracking of active methane-oxidizing communities in a landfill cover soil reveals spatial and seasonal variability. *Environmental Microbiology*. 2015;17(5):1721-37.
57. Caporaso JG, Lauber CL, Walters WA, Berg-Lyons D, Lozupone CA, Turnbaugh PJ, et al. Global patterns of 16S rRNA diversity at a depth of millions of sequences per sample. *Proceedings of the national academy of sciences*. 2011;108(Supplement 1):4516-22.

58. Apprill A, McNally S, Parsons R, Weber L. Minor revision to V4 region SSU rRNA 806R gene primer greatly increases detection of SAR11 bacterioplankton. *Aquatic Microbial Ecology*. 2015;75(2):129-37.
59. Bolyen E, Rideout JR, Dillon MR, Bokulich NA, Abnet CC, Al-Ghalith GA, et al. Reproducible, interactive, scalable and extensible microbiome data science using QIIME 2. *Nature biotechnology*. 2019;37(8):852-7.
60. Parks DH, Chuvochina M, Waite DW, Rinke C, Skarshewski A, Chaumeil P-A, et al. A standardized bacterial taxonomy based on genome phylogeny substantially revises the tree of life. *Nature biotechnology*. 2018;36(10):996-1004.
61. Chiri E, Nauer PA, Rainer E-M, Zeyer J, Schroth MH. High temporal and spatial variability of atmospheric-methane oxidation in Alpine glacier forefield soils. *Applied and environmental microbiology*. 2017;83(18).
62. Callahan BJ, McMurdie PJ, Rosen MJ, Han AW, Johnson AJA, Holmes SP. DADA2: high-resolution sample inference from Illumina amplicon data. *Nature methods*. 2016;13(7):581-3.
63. Wen X, Yang S, Liebner S. Evaluation and update of cutoff values for methanotrophic pmoA gene sequences. *Archives of microbiology*. 2016;198(7):629-36.
64. McMurdie PJ, Holmes S. phyloseq: an R package for reproducible interactive analysis and graphics of microbiome census data. *PloS one*. 2013;8(4):e61217.
65. Anderson MJ, Ellingsen KE, McArdle BH. Multivariate dispersion as a measure of beta diversity. *Ecology letters*. 2006;9(6):683-93.

## Declarations

**Acknowledgements:** This work was supported by funding from the Australian Research Council (LP160100061). We thank Roz Hagan for lab assistance, Caroline Einig for preliminary testing, Joseph Hall, Leo and Naomi Jeffrey for field assistance, Thanavit Jirapanjawat for help with DNA extractions and qPCR, and the Mid-Coast Council. LJ and DT acknowledge support from the Australian Research Council that partially funds their salaries (LP160100061 and DE180100535 respectively). CG acknowledges salary support from the National Health & Medical Research Council (APP1178715) and consumables support from the Australian Research Council (DP180101762). SA and PN are grateful for financial contributions from the University of Melbourne Research Grant Support Scheme, and PN for salary contributions from the Australian Research Council (DP180101762; awarded to CG).

**Declaration:** The authors declare no competing interests.

**Author Contributions:** SJ, DM and LJ conceived the study. LJ and DT conducted the DFM fieldwork with guidance from PN. LJ collected bark samples and conducted incubation experiments with guidance from DM and SJ. EC, CG and PML designed and conducted microbial community analysis. LJ, SJ, DM, CG and EC wrote the manuscript. All authors edited and approved the manuscript.

## Additional Information

Supplementary information is available for this paper. Correspondence and requests for materials should be addressed to LJ (luke.jeffrey@scu.edu.au). Reprints and permissions information is available at [www.nature.com/reprints](http://www.nature.com/reprints).

## Figures

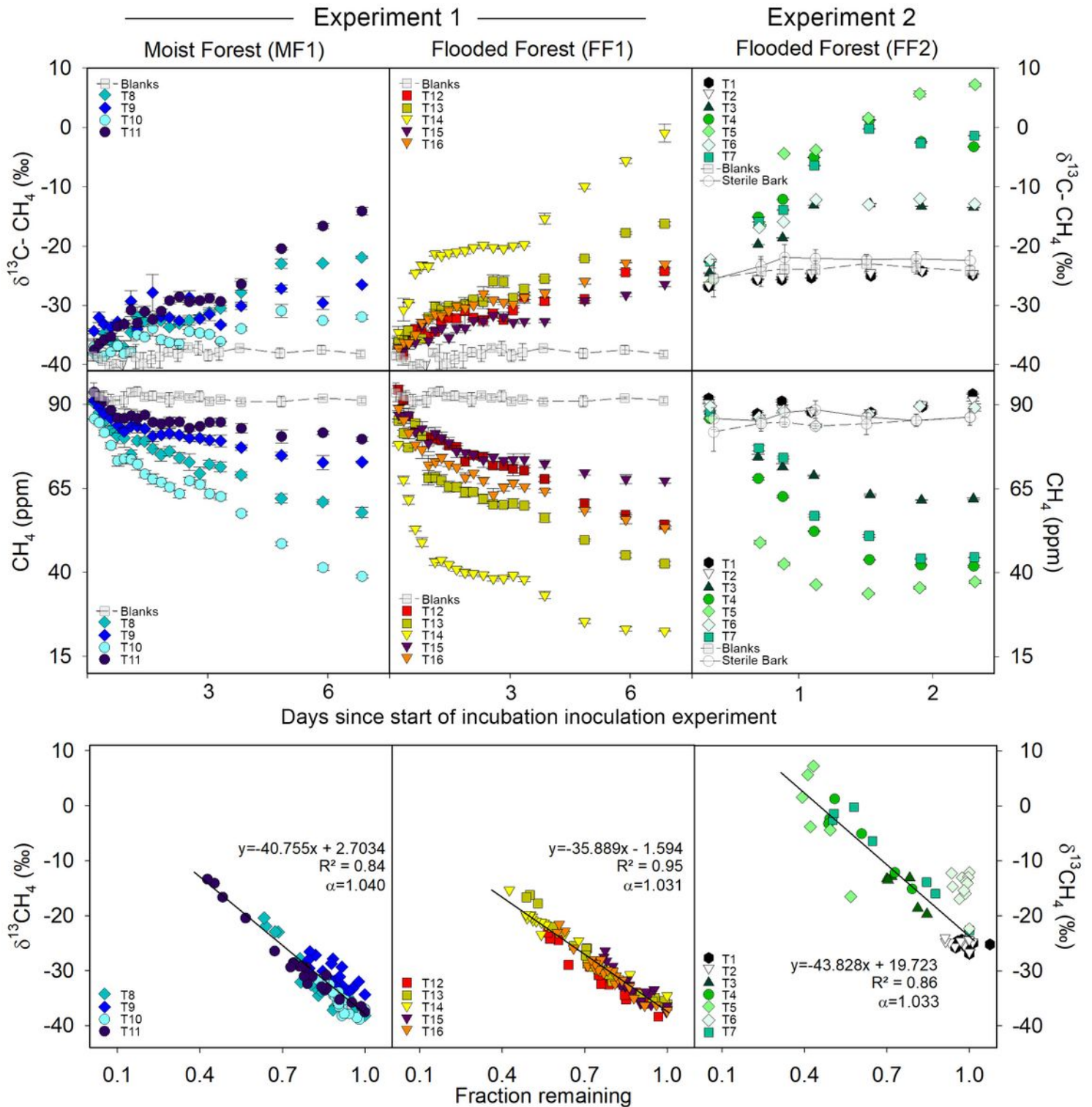


## Figure 1

MOB time series incubation experiments of methane inoculated *M. quinquenervia* bark, demonstrating oxidation as  $\delta^{13}\text{C}\text{-CH}_4$  enrichment vs time (top), decrease in methane concentration (ppm) vs time (middle), and the  $\delta^{13}\text{C}\text{-CH}_4$  vs fraction remaining (bottom). Note: Different  $\delta^{13}\text{C}\text{-CH}_4$  (‰) starting values between the first (MF, FF1) and second (FF2) experiments are due to using a different methane gas standard. Coloured symbols represent each bark sample (see Table S1, T=tree) and  $\alpha$  = fractionation factor. Average values for both controls (blank bottles and sterilised bark) are shown as grey symbols with trend line. Note: T1, T2 and T6 were removed from fraction remaining correlation due to lack of MOB oxidation, which was supported by lower MOB abundance within the paired bark samples (see microbial data in Fig. 2).

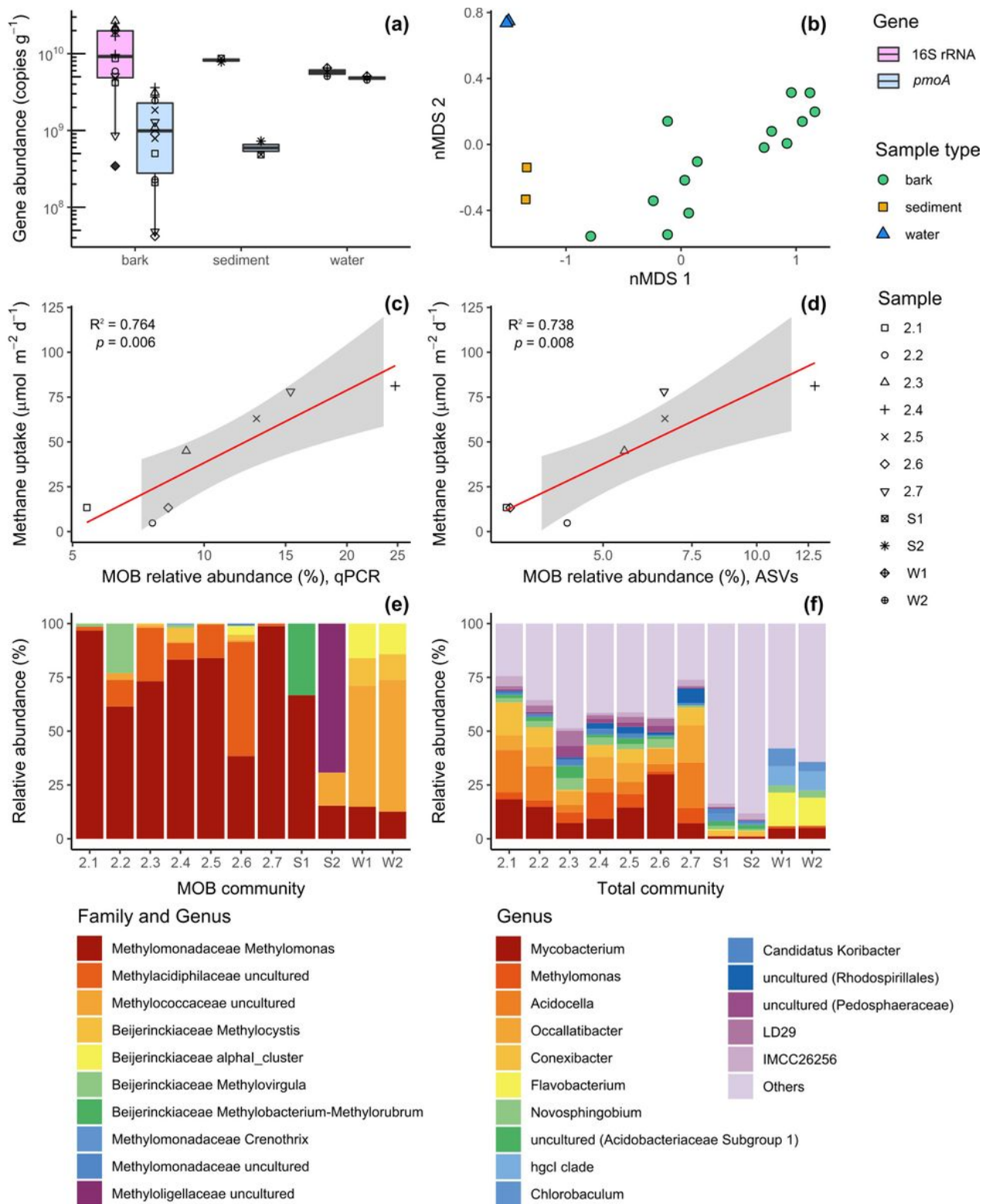


**Figure 2**

Summary of abundance, composition and structure of total microbial and methanotroph (MOB) communities in *M. quinquenervia* bark ( $n = 14$ , T = tree), sediment sample ( $n = 2$ , S = sediment) and water samples ( $n = 2$ , W = water). (a) Abundance determined by quantitative PCR of the total microbial community (universal 16S rRNA gene copy number) and of the MOB community (*pmoA* gene copy number). (b) Non-metric multidimensional scaling (nMDS) ordination of the MOB community structure

(beta diversity) measured by Bray-Curtis distance matrix of the 16S rRNA gene amplicon sequences affiliated with known methanotrophic families and genera. (c), (d) Correlation between laboratory incubation measurements of methane uptake from bark samples and logit-transformed MOB community proportion in the total community (percentage of MOB relative abundance) inferred from qPCR (c), and 16S rRNA amplicon sequence variants (d). (e) Relative abundance of methanotrophic genera identified from the analysis of the 16S rRNA gene amplicon sequences. In case of uncultured genus, taxonomic resolution according to family is reported. (f) Relative abundance of 16S rRNA gene amplicon sequences resolved at the taxonomic level of genus.

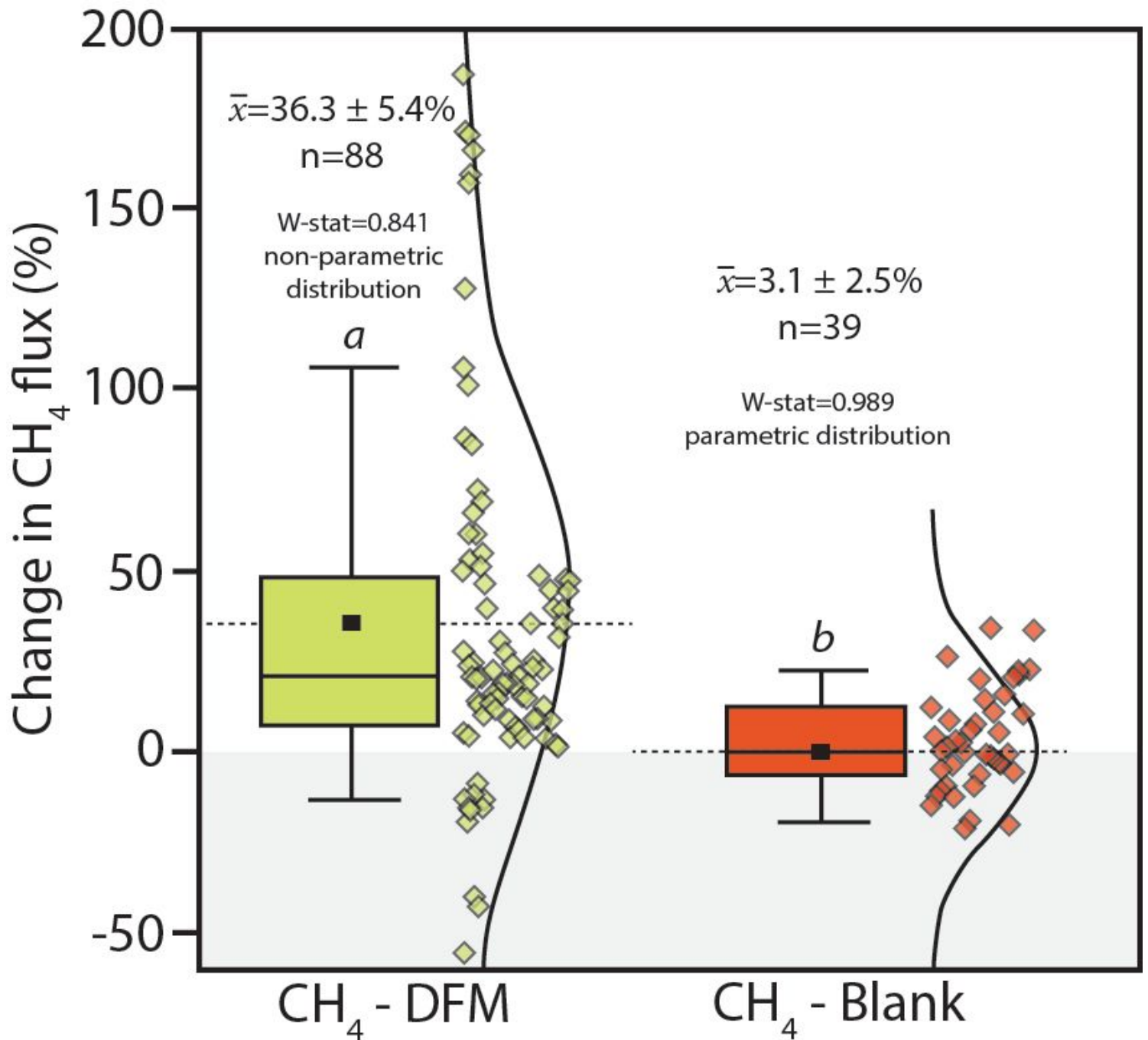


Figure 3

Summary of in situ DFM MOB inhibitor tests conducted on *M. quinquenervia* bark revealing the mostly positive % increase in methane fluxes ~1 hour after the addition of DFM and non-parametric distribution (Shapiro-Wilk, W-stat = 0.841). The blank replicates (i.e. repeated chamber measurements after ~1 hour, but no DFM addition) showed no change in mean methane fluxes ( $3.1 \pm 2.5$  %) and normal distribution (Shapiro-Wilk, W-stat = 0.989). There were significant differences between treatments a and b (ANOVA on-ranks,  $p < 0.001$ ). Note: The box represents the 25-75 percentile, error bars 1-99 percentile, the solid horizontal line is the median, dashed line and small square = mean ( $\bar{x}$ ), and the curved line and scatter plots show the data distribution.

## Supplementary Files

This is a list of supplementary files associated with this preprint. Click to download.

- [FigureS1.png](#)
- [FigureS2.png](#)
- [FigureS3.png](#)
- [SupplementaryTables.docx](#)